Observationally constrained equatorward shift of the jet streams in response to ocean warming and sea-ice loss combined

James A. Screen[1], Rosemary Eade[1,2], Doug M. Smith[2], Stephen Thomson[1] and Hao Yu[1]

[1]*Department of Mathematics, University of Exeter, Exeter, UK*

[2]*Met Office Hadley Centre, Exeter, UK*

Key points

- Antarctic and Arctic sea-ice loss cause an equatorward shift of the winter jet stream in the southern and northern hemisphere, respectively
- Models with stronger eddy feedback simulate farther jet shifts in response to both Antarctic and Arctic sea-ice loss
- Observationally constrained equatorward jet shifts due to sea-ice loss exceed in magnitude the opposing poleward shifts due to ocean warming

Plain Language Summary

Winter weather in the midlatitudes of the northern and southern hemispheres is influenced by the position of the jet streams. In a warming climate, the jet streams may move from the current average location. Past work has suggested that sea-ice loss and ocean warming affect the jet stream location in opposite directions, leading to a 'tug-of-war' on the jet. It is unclear which factor 'wins' this tug-of-war and so, in what direction the jet stream may shift in the future. We use new climate model experiments to better measure the separate effects of sea-ice loss and ocean warming on the jet streams. Antarctic and Arctic sea-ice loss cause an equatorward shift of the winter jet stream in the southern and northern hemisphere, respectively. Models tend to underestimate these jet shifts in response to sea-ice loss compared to the real world. Ocean warming causes a poleward jet shift in both hemispheres, that approximately cancel out the equatorward shifts due to sea-ice loss. However, when we account for the model underestimation of the jet shifts in response to sea-ice loss, we find that sea-ice loss 'wins' the tug-of-war, which suggests the jets move equatorward in a warmer climate.

Abstract

We examine the midlatitude jet stream responses to projected Antarctic and Arctic sea-ice loss and global ocean warming in coordinated multi-model experiments from the Polar Amplification Model Intercomparison Project. Antarctic and Arctic sea-ice loss cause an equatorward shift of the winter jet stream in the southern and northern hemisphere, respectively, on average across the models. Models with stronger eddy feedback simulate farther equatorward jet shifts in response to both Antarctic and Arctic sea-ice loss. The models simulate too weak eddy feedback compared to the real world, particularly in the northern hemisphere, resulting in an underestimation of the boreal jet response to Arctic sea-ice loss. More precise estimates of the jet shifts are obtained by using the observed eddy feedback as a constraint and suggest that the equatorward jet shifts in response to Antarctic and Arctic sea-ice loss exceed in magnitude the opposing poleward shifts due to ocean warming.

1. Introduction

Arctic sea ice has declined dramatically in response to global warming (Notz and Stroeve, 2016) and is projected to further diminish even under the most optimistic decarbonisation scenarios (Notz et al., 2020). Antarctic sea ice has been relatively stable in comparison but record lows in recent years may hint at the emergence of a downward trend (Eayrs et al., 2021) that is projected in climate models (Roach et al., 2019). Sea-ice loss enhances warming in the lower atmosphere at high latitudes (Screen and Simmonds, 2010), reducing the near-surface equator-to-pole temperature difference and potentially, affecting the midlatitude jet streams (e.g., Cohen et al., 2014; Barnes and Screen, 2015; Cohen et al., 2020).

The boreal (northern hemisphere) and austral (southern hemisphere) jets are simulated by climate models to shift equatorward and weaken in response to Arctic sea-ice loss (e.g., Screen et al., 2018; Zappa et al., 2018; Screen and Blackport, 2019; Smith et al., 2022) and Antarctic sea-ice loss (Ayres et al., 2018; England et al., 2018; Ayres et al., 2020), respectively, albeit with uncertain magnitude. Whilst many studies have examined the responses to projected Arctic and Antarctic sea-ice loss separately, there has been limited quantitative comparison of the two. One notable exception is England et al. (2018), which reported a farther equatorward shift of the boreal jet in response to Arctic sea-ice loss than of the austral jet in response to Antarctic sea-ice loss, but the austral jet slowed more in response to Antarctic sea-ice loss than did the boreal jet in response to Arctic sea-ice loss. A limitation of England et al. (2018) is its reliance on a single model.

This study provides the first multi-model comparison of the responses to Arctic and Antarctic sea-ice loss. One motivation for this comparison is to determine if the same processes contribute to model uncertainty in each hemisphere. Smith et al. (2022) showed that the boreal jet shift response to Arctic sea-ice loss was larger in models with stronger eddy feedback and introduced a method to constrain the jet response using the observed eddy feedback strength. Here, we show that eddy feedback is also the dominant cause of model uncertainty in the austral jet response to Antarctic sea-ice loss. Additionally, we expand on past work by exploring the implications of too weak eddy feedback in models for the projected tug-of-war between equatorward jet shifts in response to sea-ice loss and the opposing poleward jet shifts in responses to global sea surface temperature (SST) changes.

2. Data and Methods

We analyse output from the Polar Amplification Model Intercomparison Project (PAMIP; Smith et al., 2019). The PAMIP provides coordinated experiments performed with multiple atmospheric general circulation models using the same prescribed ocean surface boundary conditions. In the present-day control experiment (pdSST-pdSIC), observed (1979-2008 average) SST and sea ice concentrations (SIC) are prescribed globally. In the future sea ice experiments, SST is the same as pdSST-pdSIC but SIC is replaced with projected values in a world 2 °C warmer than the preindustrial average, separately in the Arctic (pdSST-futArcSIC) and Antarctic (pdSST-futAntSIC), and future SSTs are used where sea ice is lost. Conversely in the future SST experiment (futSST-pdSIC), SIC is same as pdSST-pdSIC but SST is replaced with projected values at 2 °C global warming. All experiments start on 1 April and run for 14 months, with the first two months discarded for model spin-up. Ensemble members differ only in their initial atmospheric condition. Further details on the experiment design can be found in Smith et al. (2019). Here, we use models that provided data for at least three of the four experiments and for these, use all available ensemble members for each experiment (Supplementary Table 1).

All model output was re-gridded to a common grid prior to analysis; that of the lowest resolution model, CanESM5 (~2.8 ° latitude/longitude). We focus on winter averages, defined as December, January and February for the northern hemisphere and July, August and September for the southern hemisphere. Responses are calculated as the ensemble-mean difference between the perturbation and control experiment (i.e., pdSST-futAntSIC minus pdSST-pdSIC yields the response to Antarctic sea-ice loss; pdSST-futArcSIC minus pdSST-pdSIC yields the response to Arctic sea-ice loss; futSST-pdSIC minus pdSST-pdSIC yields the response to global SST warming). For each model,

the statistical significance of a response was assessed using a two-sided Student's t-test and is reported at the 95% confidence level. Multi-model means give equal weight to each model, i.e., we averaged ensemble members for each model before averaging across models. Uncertainty in the multi-model means is indicated using the standard deviation of individual model responses, multiplied by two.

We also sampled the Coupled Model Intercomparison Project phase 6 (CMIP6; Eyring et al., 2016) historical experiments and projections, identifying 30-year time windows when the global-mean near-surface air temperature averaged 14.2 and 15.7 °C, which match the definitions of present-day and future in the PAMIP (Smith et al., 2019). We sampled from all available ensemble members and for the projections, from all available scenarios for each model (Supplementary Table 2). The CMIP6 realisations from CESM2 were supplemented by fifty members from the CESM2 large ensemble, run with CMIP6 forcing (Rodgers et al., 2021).

Jet speed and latitude were calculated as in Zappa et al. (2018) and Ayres et al. (2019). Jet latitude was calculated as the sum of latitude weighted by the square of the zonal-mean zonal wind at 850 hPa between 30 and 70 °N (or °S), and jet speed as the zonal-mean zonal wind at the grid-point latitude closest to the jet latitude. In the models, latitude is defined from -90 to 90 °N rather than 90 °S to 90 °N. For ease of interpretation, we use the absolute value of latitude so that a poleward shift is expressed as a jet latitude response greater than zero and an equatorward shift as a response less than zero, in both hemispheres.

Eddy feedback strength is estimated from the local correlation squared (i.e., the variance explained) between winter zonal-mean zonal wind and divergence of the northward Eliasson-Palm flux averaged over the mid-to-upper troposphere and midlatitudes (24–72 °N or °S, 600–200 hPa), following Smith et al. (2022). It is calculated for each model by correlating across ensemble members in the pdSST-pdSIC experiment, and for the ERA5 and JRA55 reanalyses by correlating over time. The two reanalyses gave identical values to each other (to 2 decimal places).

3. Hemispheric symmetry

Both Antarctic and Arctic sea-ice loss induce lower tropospheric warming in the middle to high latitudes (Fig. 1a, b). Polar warming extends to higher altitudes in response to Arctic than Antarctic sea-ice loss. There are regions of cooling in the midlatitude mid-to-upper troposphere in both hemispheres, which we will discuss later. There is hemispheric symmetry in the multi-model-mean zonal-mean westerly responses to Antarctic and Arctic sea-ice loss (Fig. 1c, d). Both feature weakening at ~50-65 ° and strengthening at ~30-45 °, throughout the troposphere and robust across

the models. The maximum weakening occurs on the poleward side of the climatological maximum westerly wind and the maximum strengthening on the equatorward side. The jets shift equatorward in both hemispheres, but farther in response to Arctic sea-ice loss than Antarctic sea-ice loss, consistent with the stronger and deeper Arctic warming. The multi-model mean jet shifts are -0.5 and -0.2 ° latitude for Arctic and Antarctic sea-ice loss, respectively (Fig. 3).

Although the pattern of the westerly response is broadly similar across the models, there is large variation in magnitude across the models (Fig. 2). These inter-model variations are coherent between the responses to Antarctic and Arctic sea-ice loss. There is a linear relationship (r = 0.66) between the magnitudes of the jet shifts in response to Antarctic and Arctic sea-ice loss (Fig. 3). That is, models that simulate a more equatorward shift of the austral jet in response to Antarctic sea-ice loss also tend to simulate a more equatorward shift of the boreal jet in response to Arctic sea-ice loss. This suggests that a common cause for the model uncertainty in the jet latitude responses to sea-ice loss in both hemispheres. In contrast, the jet speed responses vary less coherently between the hemispheres (Supplementary Fig. 1a).

4. Modulation by eddy feedback

Next, we explore whether eddy feedback can explain the range of modelled responses to Antarctic sea-ice loss. Across-model variation in eddy feedback strength over northern midlatitudes is strongly correlated with that over southern midlatitudes (Fig. 3b). Southern hemisphere eddy feedback strength is strongly correlated (r = -0.84) with the austral jet shift in response to Antarctic sea-ice loss: models with greater eddy feedback tend to simulate a farther equatorward jet shift (Fig. 3c). A similar relationship is seen between the northern hemisphere eddy feedback strength and the boreal jet response to Arctic sea-ice loss (Fig. 3d; r = -0.75), consistent with Smith et al. (2022). In the southern hemisphere, the observed eddy feedback strength falls in the middle of the range of modelled values and is only slightly larger than the multi-model mean (Fig. 3d). Accordingly, the constrained best estimate for the austral jet shift in response to Antarctic sea-ice loss is -0.23 [-0.34 to -0.12] ° latitude (Fig. 3d), again only slightly larger in magnitude than the unconstrained multi-model mean (Fig. 4a). However, the observational constraint narrows the uncertainty range, giving greater confidence that the austral jet shifts equatorward in response to Antarctic sea-ice loss (Fig. 4a). The observed eddy feedback is greater than in any of the models in the northern hemisphere, and 65% greater than the multi-model mean (Fig. 3d). Too weak eddy feedback has also been found in seasonal forecasting systems (Scaife et al., 2019; Hardiman et al., 2022). The constrained estimate

for the boreal jet shift in response to Arctic sea-ice loss is -0.8 [-0.51 to -0.92] ° latitude (Fig. 3d), significantly larger in magnitude than the multi-model-mean, -0.5 ° latitude (Fig. 4b).

Eddy feedback strength explains some of the model spread in the austral jet speed response to Antarctic sea-ice loss but less than for the jet shift response (Supplementary Fig. 1c). Models with stronger eddy feedback tend to simulate a larger weakening of the jet. The constrained response is -0.13 [-0.23 to -0.03] m/s compared to the multi-model mean response of -0.10 [-0.35 to 0.14] m/s. Again, the observational constraint narrows the uncertainty range to exclude zero, leading to greater confidence that the austral jet slows in response to Antarctic sea-ice loss. The boreal jet speed response to Arctic sea-ice loss is not significantly related to eddy feedback strength (Supplementary Fig. 1d).

5. Tug of war on the jet

Jet shifts in response to sea-ice loss may be offset or masked by opposite signed responses to global SST warming, often referred to as the tug-of-war between the Arctic (or Antarctic) and the tropics because sea-ice loss causes maximum warming in the polar regions and global SST warming causes greatest warming in the tropics (e.g., Barnes and Polvani, 2015; Hay et al., 2022). In the PAMIP experiments, global SST warming induces warming throughout the troposphere and at all latitudes, with maximum warming in the tropical upper troposphere and strengthened westerlies in the core and on the poleward side of the midlatitude jets in both hemispheres (Supplementary Fig. 2). Averaged across models, the poleward jet shift to Global SST warming is more than twice the magnitude in the northern hemisphere than in the southern hemisphere: 0.4 and 0.15 ° latitude (Fig. 4). Global SST warming induces a poleward jet shift in the northern hemisphere in all models, and in all-bar-one model in the southern hemisphere (Fig. 4). Like the responses to Antarctic and Arctic sea-ice loss, there is considerable model spread in the magnitudes of the jet shifts in response to global SST warming. The model spread is larger for the boreal jet shift response to global SST warming than to Arctic sea-ice loss, consistent with Hay et al. (2018), but larger for the austral jet shift response to Antarctic sea-ice loss than to global SST warming. Unlike for the responses to Antarctic and Arctic sea-ice loss however, the spread in the responses to SST is not coherent between the hemispheres and is not related to eddy feedback strength in either hemisphere (Supplementary Table 3).

Assuming the responses to sea ice and SST are linearly additive (McCusker et al., 2017; Oudar et al., 2017; Blackport and Kushner, 2017; Hay et al., 2022), the net effect of ocean surface boundary changes can be estimated by taking their sum. For the boreal jet, we use the sum of the responses

to SST and Arctic sea-ice loss and for the austral jet, we use the sum of the responses to SST and Antarctic sea-ice loss. This is because the response to Antarctic sea-ice loss is small in the northern hemisphere (relative to that to Arctic sea-ice loss and global SST warming) and the response to Arctic sea-ice loss is small in the southern hemisphere (relative to that to Antarctic sea-ice loss and global SST warming). We note these experiments lack ocean coupling, which can lead to interhemispheric responses to sea-ice loss (Deser et al., 2015); however even with an interactive ocean, these remote responses are small compared to the more local response to sea-ice loss within the respective hemisphere (England et al., 2020; Ayres et al., 2022). In almost all models and in both hemispheres, the responses to global SST warming and sea-ice loss oppose each other, and their sum is of lesser magnitude than either of them separately (Fig. 4). Their sum can be an equatorward or poleward shift, in either hemisphere, due to one response dominating over the other. Roughly half the models simulate a net poleward shift of the austral jet and the other half a net equatorward shift. Two thirds of the models simulate a net equatorward shift of the boreal jet. Considering the multi-model-mean, which might provide the best estimate of the forced response due to the large ensemble size, the net effect is close to zero in both hemispheres. Large model spread means neither the multi-model-mean austral jet latitude response to Antarctic sea-ice loss or global SST warming, or their sum, are significantly different from zero. For the boreal jet, there is an approximate cancellation of the significant equatorward shift in response to Arctic sea-ice loss by the poleward shift in response to global SST warming.

Applying the eddy feedback constraint to the responses to sea-ice loss and recalculating the sum of the responses to sea-ice and SST (we could not identify a constraint on the response to SST; see later discussion), increases the magnitude of the net equatorward shift in the boreal jet three-fold, compared to the multi-model-mean, and doubles it for the austral jet. But both start from a low baseline, so even the constrained estimates of the net responses, -0.3 and -0.1 ° latitude respectively for the boreal and austral jet, are small compared to unforced interannual variability: the standard deviation of boreal jet latitude is approximately 2.0 ° latitude and 1.2 ° latitude for the austral jet.

6. Discussion

Emergent constraints should be supported by a physical mechanism and confirmed by out-of-sample testing (Hall et al., 2019). The response to Antarctic sea-ice loss provides an out-of-sample test of the constraint proposed by Smith et al. (2022). Smith et al. (2022) provided a mechanism to physically justify using the eddy feedback strength to constrain the boreal jet shift in response to

Arctic sea-ice loss. A key aspect of their proposed mechanism was a lower tropospheric meridional overturning circulation anomaly, with ascent and adiabatic cooling on the equatorward side of the jet, and descent and adiabatic warming on the poleward side of the jet, which cause changes in eddy activity that reinforce the equatorward jet shift. Figure 1a suggests a similar mechanism for the equatorward austral jet shift in response to Antarctic sea-ice loss, with cooling identified at 35-50 °S that well matches that attributed to anomalous meridional overturning by Smith et al. (2022). Our finding that the austral jet response to Antarctic sea-ice loss is closely related to eddy feedback supports a physical and not purely statistical relationship.

The response to global SST warming is not related to eddy feedback. So, what might cause model spread in the response to global SST warming? Poleward jet shifts in response to global SST warming are understood to be related to tropical upper tropospheric warming (e.g., Harvey et al, 2014; Barnes and Polvani, 2015; Oudar et al., 2020; Hay et al., 2022). We find models that warm more in the tropical upper troposphere and have larger increases in the upper tropospheric (150-300 hPa) tropics-to-pole temperature gradient tend to simulate a more poleward boreal jet shift (Supplementary Table 3). However, no such relationship is found for the austral jet. Model uncertainty in austral jet shift has been linked to model biases in the climatological jet latitude: models with a more equatorward mean jet position tend to simulate a larger poleward shift in response to CO_2 forcing (e.g., Kidson and Gerber 2010; Bracegirdle et al., 2013; Curtis et al., 2020) but without a clear physical mechanism (Simpson and Polvani, 2016). We find a moderate correlation ($r = 0.58$; Supplementary Table 3) between the austral jet shift and the climatological jet latitude; however, it is of opposite sign to expected, not statistically significant, and a single outlier exerts a lot of leverage (not shown) and so, for these reasons, we consider the relationship to be spurious. Harvey et al. (2014) suggested the magnitude of southern hemisphere storm track shift could be explained by the upper and lower tropospheric equator-to-pole temperature difference, but neither metric can explain the model spread found here for the austral jet response to global SST warming. In short, we have been unable to identify the cause of the differing austral jet latitude responses to global SST warming.

The multi-model-mean net jet latitude responses (sum of responses to sea-ice loss and global SST warming) are not statistically different ($p = 0.16$ and 0.38 for austral and boreal jet, respectively) to the projected shifts in the CMIP6 simulations for equivalent global warming (Fig. 4). This suggests the multi-model-mean projected jet shift can be well described by the linear combination of the opposing responses to sea-ice loss and global SST warming, particularly for the boreal jet. For individual models, there are discrepancies between the net responses and those in

CMIP6, which could be due to 1) internal variability; 2) that direct radiative forcing from increased CO_2, which is not included in the PAMIP simulations, induces an additional poleward shift component (Grise and Polvani, 2014); 3) that ocean coupling, also absent in the PAMIP simulations, modulates the jet responses; 4) that the jet responses are sensitive to the pattern of SST warming (Wood et al., 2020), which differ between PAMIP and CMIP6; or 5) that the jet responses are sensitive to the model mean states (Bracegirdle et al., 2018; Curtis et al., 2020), which again differ between PAMIP and CMIP6. Factors 1, 4 and 5 may average out, leading to better agreement between PAMIP and CMIP6 for the multi-model-mean than for individual models.

7. Conclusions

Antarctic and Arctic sea-ice loss cause an equatorward shift of the austral and boreal jet stream, respectively, on average across the models. Eddy feedback strength is the dominant cause of model variation in the magnitude of the jet latitude responses to sea-ice loss in both hemispheres. Models with stronger eddy feedback simulate farther equatorward jet shifts in response to both Antarctic and Arctic sea-ice loss. The models simulate too weak eddy feedback, particularly in the northern hemisphere, resulting in an underestimation of the boreal jet latitude shift in response to Arctic sea-ice loss. We have shown that more precise estimates of the jet shifts in response to Arctic and Antarctic sea-ice loss can be obtained by using observed eddy feedback as a constraint. The constrained estimates suggest the equatorward jet shifts in response to Antarctic and Arctic sea-ice loss exceed in magnitude the opposing poleward shifts due to global SST warming. Further work is needed to better understand and constrain the jet latitude response to global SST warming. If this is accurate in models, or overestimated, or underestimated less than the jet latitude response to sea-ice loss, then jets shifts will be too far poleward in climate change projections.

Acknowledgments. We thank the modelling groups that contributed to the PAMIP and CMIP6. Aspects of this work were inspired by the CMIP6 data hackathon (Mitchell et al., 2022); we thank the organisers, and the participants of project 5 for their input. J.A.S and S.T. were funded by Natural Environment Research Council grant NE/V005855/1. D.M.S. and R.E were supported by the Met Office Hadley Centre Climate Programme funded by BEIS and Defra. H.Y. was supported by the China Scholarship Council.

Open Research. All data used in the study are freely available to download. The CMIP6 simulations, including the contribution from PAMIP, are accessible on the Earth System Grid Federation

(https://esgf-index1.ceda.ac.uk/search/cmip6-ceda/) by searching for the models ('Source ID') and experiments ('Experiment ID') as listed in Supplementary Table 1 and 2.

References

Ayres, H. C., Screen, J. A., Blockley, E. W., and Bracegirdle, T. J. (2022). The coupled atmosphere–ocean response to Antarctic sea ice loss. Journal of Climate 35(14), 4665-4685. https://doi.org/10.1175/JCLI-D-21-0918.1

Ayres, H., & Screen, J. A. (2019). Multimodel analysis of the atmospheric response to Antarctic sea ice loss at quadrupled CO2. Geophysical Research Letters, 46, 9861–9869. https://doi.org/10.1029/2019GL083653

Barnes, E. A., & Polvani, L. M. (2015). CMIP5 projections of Arctic amplification, of the North American/North Atlantic circulation, and of their relationship. Journal of Climate, 28, 5254–5271. https://doi.org/10.1175/JCLI-D-14-00589.1

Barnes, E. A., & Screen, J. A. (2015). The impact of Arctic warming on the midlatitude jetstream: Can it? Has it? Will it? Wiley Interdisciplinary Reviews: Climate Change, 6, 277–286. https://doi.org/10.1002/wcc.337

Blackport, R., & Kushner, P. J. (2017). Isolating the atmospheric circulation response to Arctic sea ice loss in the coupled climate system. Journal of Climate, 30(6), 2163-2185. https://doi.org/10.1175/JCLI-D-16-0257.1

Bracegirdle, T. J., Hyder, P., & Holmes, C. R. (2018). CMIP5 diversity in southern westerly jet projections related to historical sea ice area: Strong link to strengthening and weak link to shift. Journal of Climate, 31(1), 195–211. https://doi.org/10.1175/JCLI-D-17-0320.1

Bracegirdle, T. J., Shuckburgh, E., Sallee, J.-B., Wang, Z., Meijers, A. J. S., Burneau, N., Phillips, T., & Wilcox, L. J. (2013). Assessment of surface winds over the Atlantic, Indian and Pacific Ocean sectors of the Southern Ocean in CMIP5 models: Historical bias, forcing response, and state dependence. Journal of Geophysical Research: Atmospheres, 118, 547–562. https://doi.org/10.1002/jgrd.50153

Cohen, J., Screen, J. A., Furtado, J. C., Barlow, M., Whittleston, D., Coumou, D., Francis, J., Dethloff, K., Entekhabi, D., Overland, J., & Jones, J. (2014). Recent Arctic amplification and extreme mid-latitude weather. Nature Geoscience, 7(9), 627–637. https://doi.org/10.1038/ngeo2234

Cohen, J., Zhang, X., Francis, J., Francis, J., Jung, T., Kwok, R., et al. (2020). Divergent consensuses on Arctic amplification influence on midlatitude severe winter weather. Nature Climate Change, 10, 20–29. https://doi.org/10.1038/s41558-019-0662-y

Curtis, P. E., Ceppi, P., & Zappa, G. (2020). Role of the mean state for the Southern Hemispheric jet stream response to CO_2 forcing in CMIP6 models. Environmental Research Letters, 15, 064011. https://doi.org/10.1088/1748-9326/ab8331

Deser, C., Sun, L., Tomas, R. A., & Screen, J. (2016). Does ocean coupling matter for the northern extratropical response to projected Arctic sea ice loss? Geophysical Research Letters, 43, 2149–2157. https://doi.org/10.1002/2016GL067792

Deser, C., Tomas, R. A., & Sun, L. (2015). The role of ocean–atmosphere coupling in the zonal-mean atmospheric response to Arctic sea ice loss. Journal of Climate, 28(6), 2168–2186. https://doi.org/10.1175/JCLI-D-14-00325.1

Eayrs, C., Li, X., Raphael, M. N., & Holland, D. M. (2021). Rapid decline in Antarctic sea ice in recent years hints at future change. Nature Geoscience, 14, 460–464. https://doi.org/10.1038/s41561-021-00768-3

England, M. R., Polvani, L. M., Sun, L., & Deser, C. (2020). Tropical climate responses to projected Arctic and Antarctic sea-ice loss. Nature Geoscience, 13(4), 275–281. https://doi.org/10.1038/s41561-020-0546-9

England, M., Polvani, L., & Sun, L. (2018). Contrasting the Antarctic and Arctic atmospheric responses to projected sea ice loss in the late twenty-first century. Journal of Climate, 31(16), 6353–6370. https://doi.org/10.1175/JCLI-D-17-0666.1

Eyring, V., Bony, S., Meehl, G. A., Senior, C. A., Stevens, B., Stouffer, R. J., & Taylor, K. E. (2016). Overview of the Coupled Model Intercomparison Project Phase 6 (CMIP6) experimental design and organization. Geoscientific Model Development, 9, 1937–1958. https://doi.org/10.5194/gmd-9-1937-2016

Grise, K. M., & Polvani, L. M. (2014). The response of midlatitude jets to increased CO_2: Distinguishing the roles of sea surface temperature and direct radiative forcing. Geophysical Research Letters, 41(19), 6863–6871. https://doi.org/10.1002/2014GL061638

Hall, A., Cox, P., Huntingford, C., & Klein, S. (2019). Progressing emergent constraints on future climate change. Nature Climate Change, 9(4), 269–278. https://doi.org/10.1038/s41558-019-0436-6

Hardiman, S. C., Dunstone, N. J., Scaife, A. A., Smith, D. M., Comer, R., Nie, Y., & Ren, H-L. (2022). Missing eddy feedback may explain weak signal to noise ratios in climate predictions, npj Climate and Atmospheric Science, 5(57). https://doi.org/10.1038/s41612-022-00280-4

Harvey, B. J., Shaffrey, L. C., & Woolings, T. J. (2014). Equator-to-pole temperature differences and extra-tropical storm track responses of the CMIP5 climate models. Climate Dynamics, 43, 1171–1182. https://doi.org/10.1007/s00382-013-1883-9

Harvey, B., Cook, P., Shaffrey, L., & Schiemann, R. (2020). The response of the northern hemisphere storm tracks and jet streams to climate change in the CMIP3, CMIP5, and CMIP6 climate models. Journal of Geophysical Research: Atmospheres, 125, e2020JD032701. https://doi.org/10.1029/2020JD032701

Hay, S., Kushner, P. J., Blackport, R., & McCusker, K. E. (2018). On the relative robustness of the climate response to high-latitude and low-latitude warming. Geophysical Research Letters, 45, 6232–6241. https://doi.org/10.1029/2018GL077294

Hay, S., Kushner, P. J., Blackport, R., McCusker, K. E., Oudar, T., Sun, L., England, M., Deser, C., Screen, J. A., & Polvani, L. M. (2022). Separating the Influences of Low-Latitude Warming and Sea Ice Loss on Northern Hemisphere Climate Change, Journal of Climate, 35(8), 2327-2349. https://doi.org/10.1175/JCLI-D-21-0180.1

Kidston, J., & Gerber, E. P. (2010). Intermodel variability of the poleward shift of the austral jet stream in the CMIP3 integrations linked to biases in 20th century climatology. Geophysical Research Letters, 37, L09708. https://doi.org/10.1029/2010GL042873

McCusker, K. E., Kushner, P. J., Fyfe, J. C., Sigmond, M., Kharin, V. V., & Bitz, C. M. (2017). Remarkable separability of circulation response to Arctic sea ice loss and greenhouse gas forcing. Geophysical Research Letters, 44, 7955–7964. https://doi.org/10.1002/2017GL074327

Mitchell, D. M., Stone. E. J., Andrews, O. D., et al. (2022). The Bristol CMIP6 Data Hackathon. Weather, 77(6), 218–221. https://doi.org/10.1002/wea.4161

Notz, D., & SIMIP Community. (2020). Arctic sea ice in CMIP6. Geophysical Research Letters, 47(10), e2019GL086749. https://doi.org/10.1029/2019GL086749

Notz, D., & Stroeve, J. (2016). Observed Arctic sea-ice loss directly follows anthropogenic CO2 emission. Science, 354, 747–750. https://doi.org/10.1126/science.aag2345

Oudar, T., Cattiaux, J., & Douville, H. (2020). Drivers of the northern extratropical eddy-driven jet change in CMIP5 and CMIP6 models. Geophysical Research Letters, 47(8), e2019GL086695. https://doi.org/10.1029/2019gl086695

Oudar, T., Sanchez-Gomez, E., Chauvin, F., Cattiaux, J., Terray, L., & Cassou, C. (2017). Respective roles of direct GHG radiative forcing and induced Arctic sea ice loss on the Northern

Hemisphere atmospheric circulation. Climate Dynamics, 49, 3693–3713. https://doi.org/10.1007/s00382-017-3541-0

Roach, L. A., Dörr, J., Holmes, C. R., Massonnet, F., Blockley, E. W., Notz, D., et al. (2020). Antarctic sea ice area in CMIP6. Geophysical Research Letters, 47(9), e2019GL086729. https://doi.org/10.1029/2019GL086729

Rodgers, K. B., Lee, S.-S., Rosenbloom, N., Timmermann, A., Danabasoglu, G., Deser, C., et al. (2021). Ubiquity of human-induced changes in climate variability. Earth System Dynamics, 12(4), 1393– 1411. https://doi.org/10.5194/esd-12-1393-2021

Scaife, A. A., Camp, J., Comer, R., Davis, P., Dunstone, N., Gordon, M., et al. (2019). Does increased atmospheric resolution improve seasonal climate predictions? Atmospheric Science Letters, 20, e922. https://doi.org/10.1002/asl.922

Screen, J. A., & Blackport, R. (2019). How robust is the atmospheric response to projected Arctic sea-ice loss across climate models? Geophysical Research Letters, 46, 11406–11415. https://doi.org/10.1029/2019gl084936

Screen, J. A., & Simmonds, I. (2010). The central role of diminishing sea ice in recent Arctic temperature amplification. Nature, 464(7293), 1334–1337. https://doi.org/10.1038/nature09051

Screen, J. A., Deser, C., Smith, D. M., Zhang, X., Blackport, R., Kushner, P. J., Oudar, T., McCusker, K. E., & Sun, L. (2018). Consistency and discrepancy in the atmospheric response to Arctic sea-ice loss across climate models. Nature Geoscience, 11(3), 155–163. https://doi.org/10.1038/s41561-018-0059-y

Simpson, I. R., & Polvani, L. M. (2016). Revisiting the relationship between jet position, forced response, and annular mode variability in the southern midlatitudes. Geophysical Research Letters, 43, 2896–2903. https://doi.org/10.1002/2016GL067989

Smith, D. M., Screen, J. A., Deser, C., Cohen, J., Fyfe, J. C., García-Serrano, J., Jung, T., Kattsov, V., Matei, D., Msadek, R., Peings, Y., Sigmond, M., Ukita, J., Yoon, J.-H., & Zhang, X. (2019). The Polar Amplification Model Intercomparison Project (PAMIP) contribution to CMIP6: Investigating the causes and consequences of polar amplification. Geoscientific Model Development, 12, 1139–1164. https://doi.org/10.5194/gmd-12-1139-2019

Smith, D.M., Eade, R., Andrews, M.B., Ayres, H., Clark, A., Chripko, S., et al. (2022). Robust but weak winter atmospheric circulation response to future Arctic sea ice loss. Nature Communications, 13, 727. https://doi.org/10.1038/s41467-022-28283-y

Wood, T., McKenna, C. M., Chrysanthou, A., & Maycock, A. C. (2020). Role of sea surface temperature patterns for the Southern Hemisphere jet stream response to CO_2 forcing. Environmental Research Letters, 16(1), 014020. https://doi.org/10.1088/1748-9326/abce27

Zappa, G., Pithan, F., & Shepherd, T. G. (2018). Multimodel evidence for an atmospheric circulation response to Arctic sea ice loss in the CMIP5 future projections. Geophysical Research Letters, 45, 1011–1019. https://doi.org/10.1002/2017GL076096

Figures

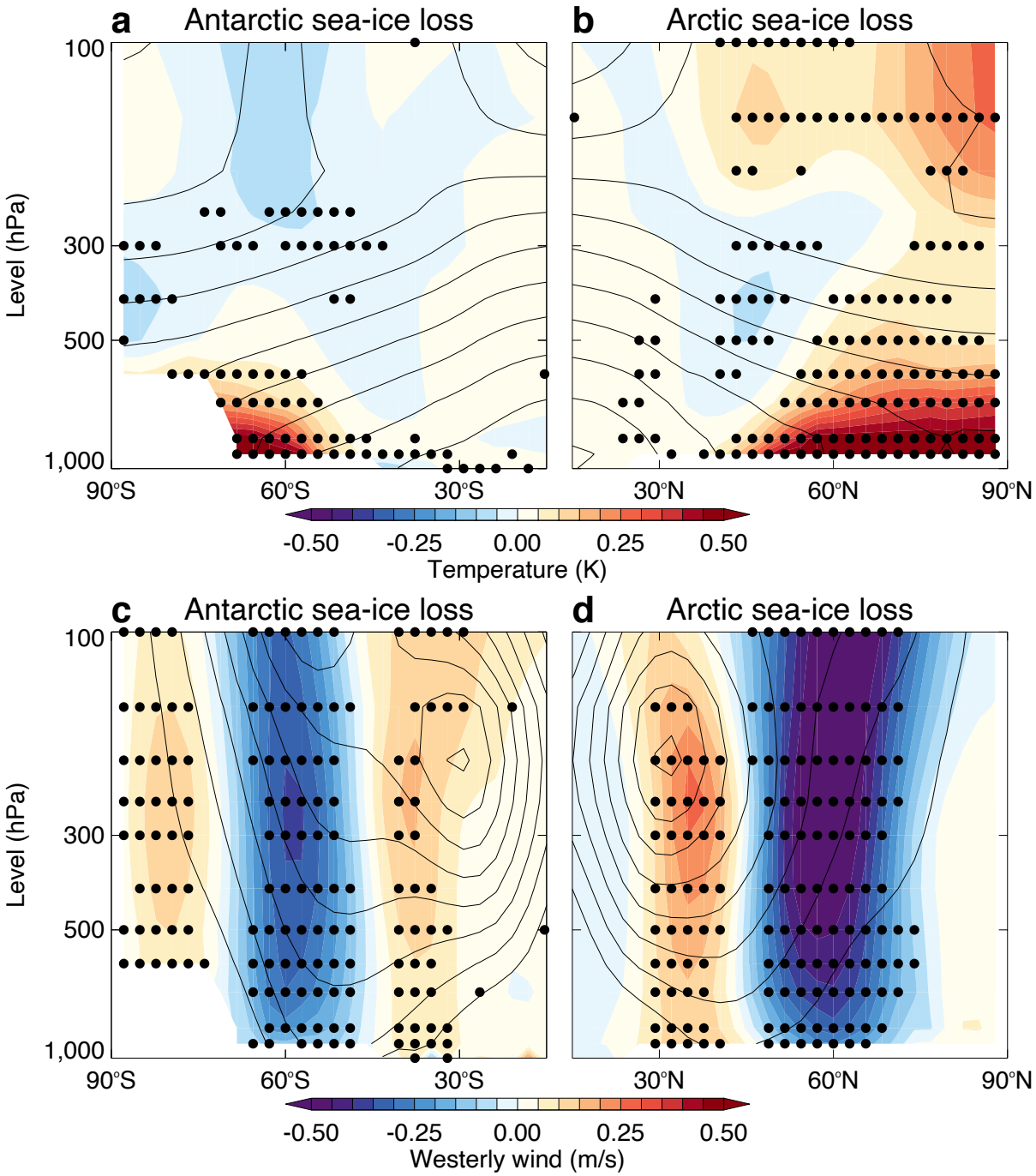

Figure 1. Hemispheric symmetry in the responses to Antarctic and Arctic sea-ice loss. Multi-model-mean winter zonal-mean air temperature response to future Antarctic sea-ice loss (**a**) and future Arctic sea-ice loss (**b**). Multi-model-mean winter zonal-mean westerly wind response to future Antarctic sea-ice loss (**c**) and future Arctic sea-ice loss (**d**). Black contours show the multi-model-mean climatology in the present-day experiment. Black dots denote that at least 80% of the models have same signed response.

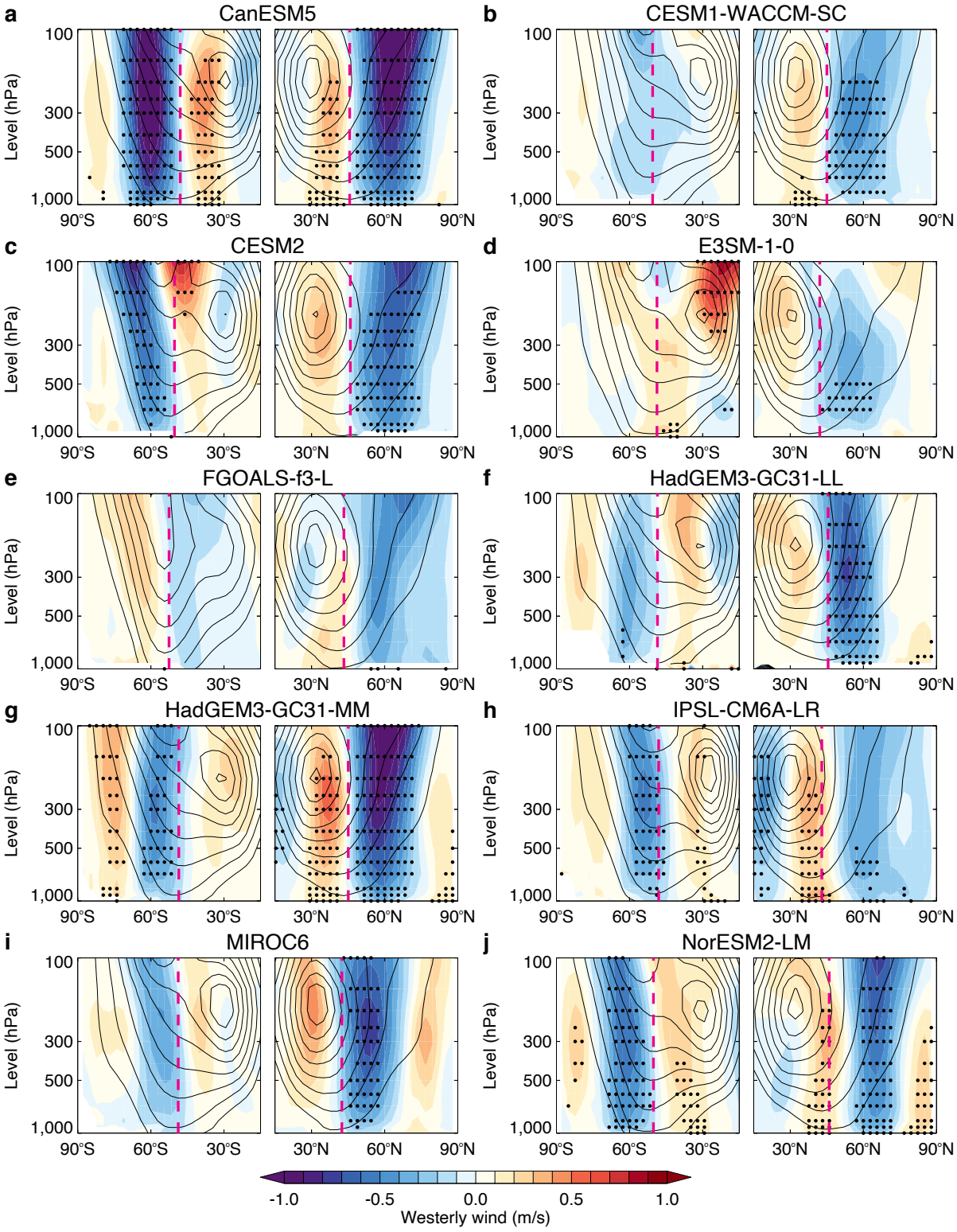

Figure 2. Responses to Antarctic and Arctic sea-ice loss coherently vary in magnitude across models. Winter zonal-mean westerly wind response (shading) to future Antarctic (left sub-panels) and Arctic (right sub-panels) sea-ice loss in ten models (**a-j**). Black contours show the wind climatology in the present-day experiment. Black dots denote a statistically significant ensemble-mean response (95% confidence). Vertical dashed magenta lines show the mean jet latitude.

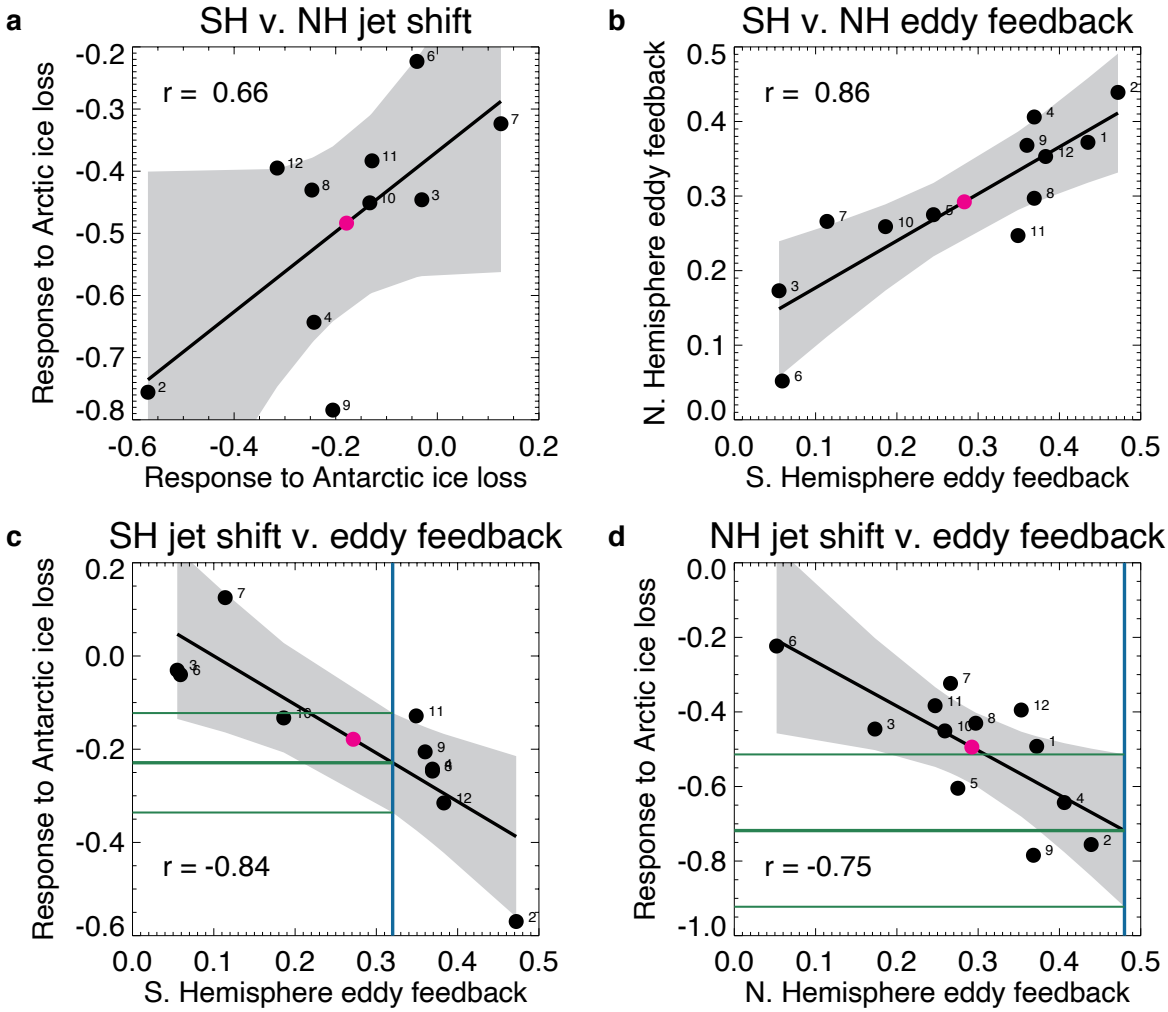

Figure 3. Eddy feedback modulates the jet response to sea-ice loss in both hemispheres. Relationships across models (black dots, numbered as in Supplementary Table 1) between the jet shifts (° poleward) in response to Antarctic and Arctic sea-ice loss (**a**); between the northern and southern Hemisphere eddy feedback (**b**); between the austral jet shift in response to Antarctic sea-ice loss and southern hemisphere eddy feedback (**c**); and between the boreal jet shift in response to Arctic sea-ice loss and northern hemisphere eddy feedback (**d**). The Pearson correlation coefficient (r) is provided. Grey shading denotes the 95% confidence intervals on the linear fit, which is shown by the black line. The vertical blue line denotes the observed eddy feedback strength, which is used to constrain the response to sea-ice loss and its uncertainty, which are shown in thick and thin green horizontal lines, respectively. The multi-model-mean is shown by an unnumbered magenta dot.

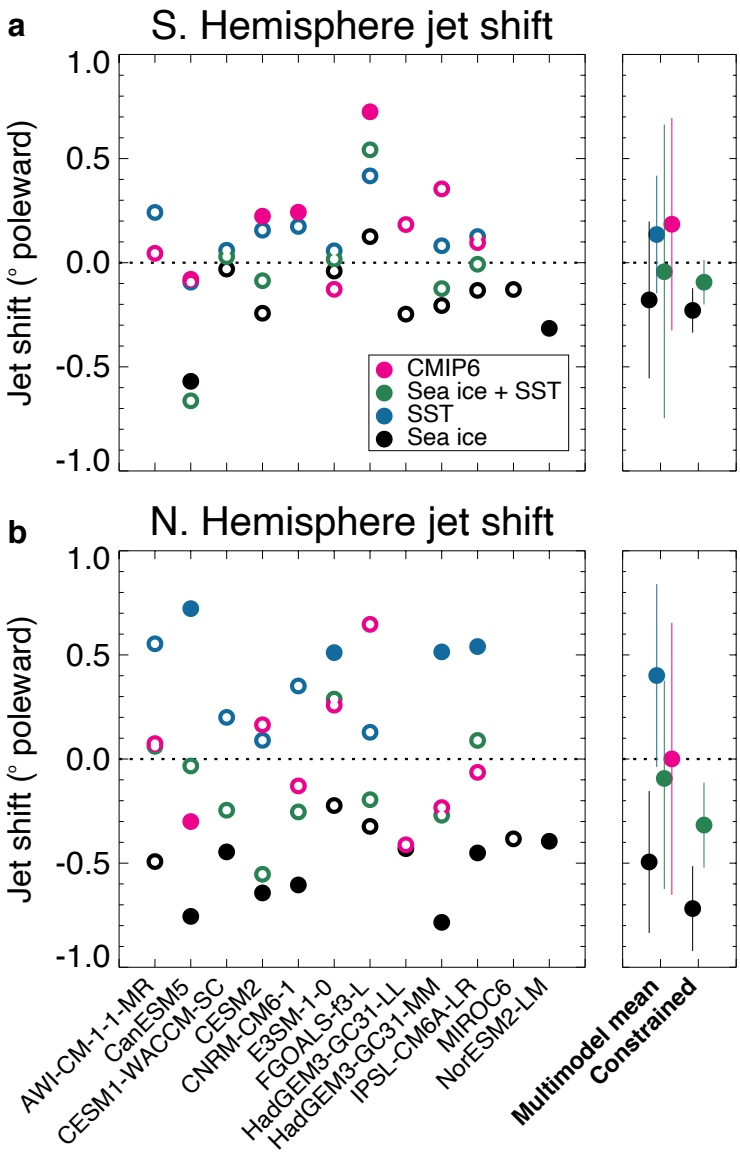

Figure 4. Jet latitude response to sea-ice loss and global SST warming. Jet latitude response (° poleward) to sea-ice loss (black circles), global SST warming (blue circles), and their sum (green circles) for each model, for the austral jet (**a**) and boreal jet (**b**). Magenta circles show the jet latitude changes simulated in CMIP6 experiments. Statistically significant (95% confidence) individual model responses are shown by filled circles; otherwise, circles are unfilled. The two rightmost panels show the multi-model-mean responses and the constrained responses, and their 95% confidence intervals.